AIMS Mathematics, 11(6): 16811–16836.
DOI: 10.3934/math.2026690
Received: 13 March 2026
Revised: 14 May 2026
Accepted: 03 June 2026
Published: 11 June 2026

https://www.aimspress.com/journal/Math

Research article

Texture enhancement of skin lesion images via Hankel determinants of λ-generalized Sakaguchi type functions in symmetric domain

Bushra Kanwal[1,*], Kashaf Fatima[1], Dalal Alhwikem[2,*] and Sheza El-Deeb[2,3]

[1] Department of Mathematical Sciences, Fatima Jinnah Women University, The Mall Rawalpindi, Pakistan

[2] Department of Mathematics, College of Science, Qassim University, Buraydah, 51452, Saudi Arabia

[3] Department of Mathematics, Faculty of Science, Damietta University, New Damietta, 34517, Egypt

* **Correspondence:** Email: bushra.kanwal@fjwu.edu.pk, d.alhwikem@qu.edu.sa.

Abstract: Digital image processing is essential in fields such as medical imaging, satellite imagery, and autonomous vehicles. Besides its applications, texture enhancement is vital for improving image visibility while preserving geometric structure. To improve visual clarity and image texture, we introduced a novel algorithm for texture enhancement. Initially, we determined coefficient inequalities of $\mathcal{S}^*(\varphi_H)$ which is a subclass of λ- generalized Sakaguchi type functions, and examined upper bounds of second and third order Hankel determinants and obtained sharp results. We proposed a texture enhancement algorithm that utilized convolution masks derived from Hankel determinants with the pixels of segmented image. This approach provided a mathematical tool for computer-aided dermatological analysis, which was used to enhance lesion boundaries and structural visibility in dermascopic images. Image quality was evaluated using different quality metrics like contrast, correlation, energy, homogeneity, and entropy. The experimental results demonstrated uniform texture enhancement and improved edge preservation in all directions. Comparative analysis showed the efficacy of our proposed algorithm compared to existing methods reported in this study, proving it suitable to enhance image quality.

Keywords: λ-generalized Sakaguchi type functions; image edge detection; Hankel determinant; algorithms; texture enhancement; medical imaging
Mathematics Subject Classification: 30C45, 30C50

1. Introduction

Analytic and univalent functions have strong geometric properties and serve in practical problems such as conformal mapping-dynamic flow. Several subclasses of analytic and univalent functions, including starlike- and convex functions, have been examined due to their geometric properties [1].

Hankel determinants play a vital role in analyzing the behavior of coefficients of univalent functions. Poomerenke [2] gave the concept of Hankel determinants, which was later examined by Noonan and Thomas [3].

In this paper, we determine second and third order Hankel determinants for a subclass of λ-generalized Sakaguchi-type functions associated with an image domain of $\varphi_H(z)$ [4]. We present basic definitions that will serve as a framework for our fundamental results.

Let class $\mathcal{A}$ be a normalized analytic functions f in an open unit disk $\mathfrak{D}$ with normalized condition $f(0) = 0$ and $f'(0) = 1$. Taylor series representation of this function is as follows:

$$f(z) = z + \sum_{n=2}^{\infty} r_n z^n, \quad \forall z \in \mathfrak{D}. \tag{1.1}$$

Two important subclasses of univalent function $\mathcal{K}$, including starlike $\mathcal{S}^*$ and convex domain $\mathcal{C}$, mapping the open unit disc $\mathfrak{D}$ onto starlike and convex domains, respectively [5]. Mathematically, we can define the classes of $\mathcal{C}$ and $\mathcal{S}^*$as follows:

$$\mathcal{C} = \left\{ f \in \mathcal{K} : \mathfrak{R}\left(\frac{(zf'(z))'}{f'(z)}\right) > 0, \quad z \in \mathfrak{D} \right\}, \tag{1.2}$$

$$\mathcal{S}^* = \left\{ f \in \mathcal{K} : \mathfrak{R}\left(\frac{zf'(z)}{f(z)}\right) > 0, \quad z \in \mathfrak{D} \right\}. \tag{1.3}$$

Littlewood [6] and Rogosinski [7] introduced distortion results for numerous subclasses of univalent functions. Subordination is the tool used to derive sharp coefficient bounds. An analytic function h is subordinate to analytic function l, denoted by $h(z) \prec l(z)$ if and only if there exists a Schwarz function $\omega(z)$ satisfying $\omega(0) = 0$, $|\omega(z)| < 1$, such that $h(z) = l(\omega(z)), \quad \forall z \in \mathfrak{D}$. The class of Caratheodary functions, [8] denoted by $\mathcal{P}$, satisfies $p(0) = 1$ and $\mathfrak{R}(p(z)) > 0$, $\forall z \in \mathfrak{D}$. The series representation of the Caratheodory function is

$$p(z) = 1 + \sum_{n=1}^{\infty} c_n z^n, \quad \forall z \in \mathfrak{D}. \tag{1.4}$$

In geometric function theory, Hankel determinants have a significant importance in examining the behavior of coefficients of analytic functions [9]. Pommerenke [2] gave the idea of Hankel determinants. A function $f(z)$ defined in Eq (1.1) has the form of Hankel determinant defined as:

$$|\mathcal{H}_{m,n}(f)| = \begin{vmatrix} r_n & r_{n+1} & \cdots & r_{n+m-1} \\ r_{n+1} & r_{n+2} & \cdots & r_{n+m} \\ \vdots & \vdots & \ddots & \vdots \\ r_{n+m-1} & r_{n+m} & \cdots & r_{n+2m-2} \end{vmatrix} \tag{1.5}$$

with $m, n \in \mathbb{N} = \{1, 2, 3, \dots\}$. For $m = 2$ and $n = 1$, the determinant is

$$|\mathscr{H}_{2,1}(f)| = \begin{vmatrix} r_1 & r_2 \\ r_2 & r_3 \end{vmatrix} = |r_3 - r_2^2|, \tag{1.6}$$

where $r_1 = 1$, and its modified formula is

$$|r_3 - \rho r_2^2|,$$

where ρ is a real number.

For $m = 2$ and $n = 2$, the second Hankel determinant is defined as:

$$|\mathscr{H}_{2,2}(f)| = \begin{vmatrix} r_2 & r_3 \\ r_3 & r_4 \end{vmatrix} = |r_2 r_4 - r_3^2|, \tag{1.7}$$

For $m = 3$ and $n = 1$, the third Hankel determinant is defined as:

$$|\mathscr{H}_{3,1}(f)| = \begin{vmatrix} r_1 & r_2 & r_3 \\ r_2 & r_3 & r_4 \\ r_3 & r_4 & r_5 \end{vmatrix} = r_3(r_2 r_4 - r_3^2) - r_4(r_4 - r_2 r_3) + r_5(r_3 - r_2^2). \tag{1.8}$$

Definition 1.1. The class $\mathcal{S}^*(\lambda)$, known as the linear combination of functions that maps the open unit disk $\mathfrak{D}$ onto a bounded turning domain and a symmetric starlike domain [4], is defined as

$$\mathcal{S}^*(\lambda) = \left\{ f \in \mathcal{K} : (1-\lambda)(f'(z))^{1-\lambda} + \lambda \left(\frac{2zf'(z)}{f(z) - f(-z)} \right)^{\lambda} \prec \varphi_H(z), \forall z \in \mathfrak{D} \right\}, \tag{1.9}$$

where $\varphi_H(z) = 1 + z + \frac{z^2}{3} - \frac{z^3}{9}$ was introduced by Lupas et al. [10]. This function maps $\mathfrak{D}$ onto image domain of $\varphi_H(z)$. We define $\mathcal{S}^*(\lambda) = \mathcal{S}^*(\varphi_H)$ as the subclass of λ-generalized Sakaguchi-type functions linked with the image domain of $\varphi_{H(z)}$.

2. Literature review

Hankel determinants have played a vital role in finding the relationship of coefficient bound and latest innovations in geometric function theory. Many researchers have focused on investigating this. For example, Shi et al. [11] investigated sharp upper bound of second order Hankel determinant of logarithmic coefficients in class S_e^* with exponential function. Shakir et al. [12] established a new coefficient bound for bi-univalent function associated with crescent shaped domain. They also found third order Hankel determinants and obtained sharp results.

Researchers have also explored the concept of convex and starlike functions. For example, Sim et al. [13] derived an upper bound for second order Hankel determinant for q-starlike functions subordinated with class $\varphi_q(\tau)$. Riaz et al. [14] found the upper bound of second and third order Hankel determinants for starlike and convex functions associated with sigmoid function and obtained sharp results. Khan et al. [15] also investigated sharp results of radius of convexity of order δ and obtained convolution properties using the Hadamard product. They proved that under some specific condition, the integral operator maps $\mathrm{BS}(\mu)$ into the family of starlike function and Libera operator maps $\mathrm{KS}(\mu)$ into the class of convex functions.

Researchers have worked on significant applications of geometric function theory in the field of image processing theory. Sivagami [16] proposed estimated coefficient bounds derived of specialized

subclass of Sakaguchi type functions to enhance the image. Priya Hari [17] used coefficient bounds derived from Sakaguchi type functions defined in the limacon shaped domain to investigate optimal gamma values and enhanced visualization tools for better detection. Kamali et al. [18] used the coefficient estimates calculated from the Quasi-Subordination class to create edge detection algorithms. For the first time, Kanwal et al. [19] used the convolution of 4 mask windows of Hankel determinants for image enhancement, and we extend this Hankel determinant approach for texture enhancement of skin lesions, utilizing 8 mask windows of Hankel determinants and achieving the best enhancement behavior.

Aldi et al. [20] developed a K-mean clustering algorithm for six types of skin cancer and extracted texture features using the Gray Level Co-occurence Matrix (GLCM) but could not produce sharp edges and best quality of image. Our proposed algorithm used convolution mask of Hankel determinants to obtain an enhanced image.

Here, we develop a novel texture enhancement algorithm that utilizes the convolution of mask windows of a Hankel determinant from λ- generalized Sakaguchi type functions linked with the image domain of $\varphi_H(z)$ with segmented image pixels through a 3×3 mask window .

3. Preliminaries

Lemma 3.1. *[21] Let $p \in \mathcal{P}$, given in* (1.4)*. Then,*

$$|c_n| \leq 2, \quad \forall n \geq 1. \tag{3.1}$$

Lemma 3.2. *[21] Let $p \in \mathcal{P}$ be given by* (1.4)*. Then,*

$$|c_{n+k} - \theta c_n c_k| \leq 2 \; max \; \{1, |2\theta - 1|\} = \begin{cases} 2, & for \; 0 \leq \theta \leq 1; \\ 2|2\theta - 1|, & otherwise. \end{cases} \tag{3.2}$$

Lemma 3.3. *[22, 23] Let $p \in \mathcal{P}$, as given by* (1.4)*. Then, if $Q \in [0, 1]$ with $Q(2Q - 1) \leq Q \leq T$, we have*

$$|c_3 - 2Qc_1c_2 + Tc_1^3| \leq 2. \tag{3.3}$$

Lemma 3.4. *[23–25] Let $p \in \mathcal{P}$, be in the form* (1.4)*. Then, for $x, y \in \mathfrak{D}$, we have*

$$2c_2 = c_1^2 + x(4 - c_1^2), \tag{3.4}$$

$$4c_3 = c_1^3 + 2c_1x(4 - c_1^2) - c_1x^2(4 - c_1^2) + 2(4 - c_1^2)(1 - |x|^2)\delta, \tag{3.5}$$

$$\begin{aligned} 8c_4 =& c_1^4 + (4 - c_1^2)x\left[c_1^2(x^2 - 3x + 3) + 4x\right] \\ & - 4(4 - c_1^2)(1 - |x|^2)\left[c(x - 1)\delta + \bar{x}\delta^2 - (1 - |\delta|^2)\rho\right]. \end{aligned} \tag{3.6}$$

Lemma 3.5. *[26] Let α, β, γ, and u satisfy $u, \alpha \in (0, 1)$ and*

$$\begin{aligned} & 8u(1 - u)[(\zeta\eta - 2\gamma)^2 + (\alpha(u + \zeta) - \eta)^2] + \zeta(1 - \zeta)(\eta - 2u\zeta)^2 \\ & \leq 4u\zeta^2(1 - \zeta)^2(1 - u). \end{aligned} \tag{3.7}$$

If $p \in \mathcal{P}$, is in the form (1.4)*. Then,*

$$|\gamma c_1^4 + uc_2^2 + 2\zeta c_1c_3 - \frac{3}{2}\eta c_1^2c_2 - c_4| \leq 2. \tag{3.8}$$

4. Main results

Theorem 4.1. *Let $f \in \mathcal{A}$ be given in* (1.1). *If $f \in \mathcal{S}^*(\varphi_H)$, then the coefficients r_2,r_3,r_4, and r_5 are*

$$\begin{aligned} |r_2| &\leq \frac{1}{2(1-2\lambda+2\lambda^2)}, \\ |r_3| &\leq \frac{1}{[3(1-\lambda)^2+2\lambda^2]}, \\ |r_4| &\leq \frac{1}{4[(1-\lambda)^2+\lambda^2]}, \\ |r_5| &\leq \frac{1}{[5(1-\lambda)^2+4\lambda^2]}. \end{aligned} \tag{4.1}$$

These inequalities are the best possible.

Proof. Let $f \in \mathcal{S}^*(\varphi_H)$. Then the Schwarz function from (1.9) can be written as

$$(1-\lambda)\left(f'(z)\right)^{1-\lambda} + \lambda\left[\frac{2zf'(z)}{f(z)-f(-z)}\right]^{\lambda} = 1 + w(z) + \frac{(w(z))^2}{3} - \frac{(w(z))^3}{9}.$$

If $l \in p$, then it can be written as in the form of the Schwarz function as

$$\begin{aligned} \hbar(z) &= \frac{1+w(z)}{1-w(z)} = 1 + c_1 z + c_2 z^2 + c_3 z^3 + \ldots \\ w(z) &= \frac{1}{2}c_1 z + (\frac{1}{2}c_2 - \frac{1}{4}c_1^2)z^2 + (\frac{1}{8}c_1^3 - \frac{1}{2}c_1 c_2 + \frac{1}{2}c_3) \\ &\quad + (\frac{1}{2}c_4 - \frac{1}{2}c_1 c_3 - \frac{1}{4}c_2^2 - \frac{1}{16}c_1^4 + \frac{3}{8}c_1^2 c_2)z^4 + \ldots \end{aligned} \tag{4.2}$$

By using (1.1), we get

$$\begin{aligned} &(1-\lambda)\left(f'(z)\right)^{1-\lambda} + \lambda\left[\frac{2zf'(z)}{f(z)-f(-z)}\right]^{\lambda} \\ &= 1 + \left[2(1-2\lambda+2\lambda^2)r_2\right]z \\ &\quad + \left\{\left[3(1-\lambda)^2+2\lambda^2\right]r_3 - \left[2\lambda(1-\lambda)\right]r_2^2\right\}z^2 \\ &\quad + \left\{4(1-2\lambda+2\lambda^2)r_4 - 2\lambda(3-3\lambda+\lambda^2)r_2 r_3 \right. \\ &\qquad \left. + \frac{4\lambda(1-\lambda)(1+2\lambda-2\lambda^2)}{3}r_2^3\right\}z^3 \\ &\quad + \cdots \end{aligned} \tag{4.3}$$

By using (4.2) and after some simplifications, we get

$$\begin{aligned} 1 + w(z) + \frac{(w(z))^2}{3} - \frac{(w(z))^3}{9} &= 1 + \frac{1}{2}c_1 z + \left(\frac{1}{2}c_2 - \frac{1}{6}c_1^2\right)z^2 \\ &\quad + \left(\frac{1}{2}c_3 - \frac{1}{3}c_1 c_2 + \frac{1}{36}c_1^3\right)z^3 \\ &\quad + \left(\frac{1}{2}c_4 - \frac{1}{3}c_1 c_3 - \frac{1}{6}c_2^2 - \frac{1}{24}c_1^2 c_2 + \frac{1}{48}c_1^4\right)z^4. \end{aligned} \tag{4.4}$$

Now, comparing (4.3) and (4.4), we get

$$r_2 = \frac{1}{4(1-2\lambda+2\lambda^2)}c_1, \tag{4.5}$$

$$r_3 = \frac{\left(\frac{1}{2}c_2 - \frac{1}{6}c_1^2\right) + \left(\frac{2\lambda(1-\lambda)}{16(1-2\lambda+2\lambda^2)^2}\right)c_1^2}{3(1-\lambda)^2+2\lambda^2}, \tag{4.6}$$

$$\begin{aligned} r_4 = \frac{1}{[4(1-\lambda)^2+\lambda^2]}\Bigg[&\frac{1}{2}c_3 + \left(\frac{8\lambda^4-17\lambda^3-17\lambda^2+33\lambda-12}{12(1-2\lambda+2\lambda^2)(3(1-\lambda)^2+2\lambda^2)}\right)c_1c_2 \\ &+\left(\frac{1}{36}+\frac{4\lambda(48\lambda^6-110\lambda^5+85\lambda^4-\lambda^3-61\lambda^2+50\lambda-15)}{192(1-2\lambda+2\lambda^2)^3(3(1-\lambda)^2+2\lambda^2)}\right)c_1^3\Bigg], \end{aligned} \tag{4.7}$$

$$r_5 = \frac{1}{D_5}\left[\frac{1}{2}c_4 + Ac_1c_3 + Bc_2^2 + Cc_1^2c_2 + Fc_1^4\right], \tag{4.8}$$

where,

$$D_5 = \frac{1}{5(1-\lambda)^2+4\lambda^2},$$

$$A = \frac{\lambda(1-\lambda)}{(1-2\lambda+2\lambda^2)},$$

$$B = \left(\frac{\frac{9}{2}\lambda(1-\lambda)-5\lambda^2+\frac{5}{2}\lambda^3}{4(3-\lambda^2)^2} - \frac{1}{6}\right),$$

$$\begin{aligned} C = &\frac{\lambda(1-\lambda)(8\lambda^4-17\lambda^3-17\lambda^2+33\lambda-12)}{6A^2(3-\lambda^2)} + \frac{3\lambda(1-\lambda)}{4A^2} \\ &- \frac{1}{2(3-\lambda^2)^2} + \frac{-6\lambda-6\lambda^2+22\lambda^3-10\lambda^4}{32A^2(3-\lambda^2)}, \end{aligned}$$

$$\begin{aligned} F = &\frac{\lambda(1-\lambda)+\lambda^2(1-\lambda)(48\lambda^6-110\lambda^5+85\lambda^4-\lambda^3-61\lambda^2+50\lambda-15)}{24A^4(3-\lambda^2)} \\ &+ \frac{\left(\frac{2}{3}\lambda-5\lambda^2+\frac{2}{3}\lambda^3\right)\left(\frac{4A^2}{3\lambda(1-\lambda)}-1\right)^2}{4(3-\lambda^2)^2}. \end{aligned}$$

Implementing (3.1) in (4.5), we get

$$|r_2| \leq \frac{1}{2(1-2\lambda+2\lambda^2)}, \tag{4.9}$$

from (4.6)

$$r_3 = \frac{\frac{1}{2}c_2 + \left(-\frac{1}{6}+\frac{2\lambda(1-\lambda)}{16(1-2\lambda+2\lambda^2)^2}\right)c_1^2}{3((1-\lambda)^2+2\lambda^2)},$$

$$r_3 = \frac{\frac{1}{2}c_2 + \left(-\frac{1}{6} + \frac{\lambda(1-\lambda)}{8(1-2\lambda+2\lambda^2)^2}\right)c_1^2}{3((1-\lambda)^2+2\lambda^2)},$$

$$r_3 = \frac{\frac{1}{2}\left(c_2 - \left(\frac{1}{3} + \frac{\lambda(1-\lambda)}{4(1-2\lambda+2\lambda^2)^2}\right)\right)c_1^2}{3((1-\lambda)^2+2\lambda^2)}.$$

Applying (3.2) in (4.6), and since $\lambda \in [0,1]$, we have

$$|r_3| \leq \frac{1}{3((1-\lambda)^2+2\lambda^2)}. \tag{4.10}$$

Rearranging (4.7), we get

$$|r_4| \leq \frac{1}{4[(1-\lambda)^2+\lambda^2]}\left[\frac{1}{2}\left|c_3 - 2Qc_1c_2 + Tc_1^3\right|\right],$$

where,

$$Q = \frac{-\left(8\lambda^4 - 17\lambda^3 - 17\lambda^2 + 33\lambda - 12\right)}{12(1-2\lambda+2\lambda^2)(3(1-\lambda)^2+2\lambda^2)},$$

$$T = \frac{1}{18} + \frac{P(\lambda)}{24(1-2\lambda+2\lambda^2)^3(3(1-\lambda)^2+2\lambda^2)},$$

using (3.3), we get

$$|r_4| \leq \frac{1}{4[(1-\lambda)^2+\lambda^2]}, \tag{4.11}$$

from (4.8), we get

$$r_5 = \frac{1}{D_5}\left[\frac{1}{2}c_4 + Ac_1c_3 + Bc_2^2 + Cc_1^2c_2 + Fc_1^4\right],$$

$$|r_5| = \frac{1}{2D_5}\left|c_4 + 2Ac_1c_3 + 2Bc_2^2 + 2Cc_1^2c_2 + 2Fc_1^4\right|,$$

by comparing (3.8), we get

$$A = \zeta, 2B = u, 2F = \gamma, 2C = -\frac{3}{2}\eta.$$

Substituting these values into (3.7),

$$(\zeta\eta - 2\gamma)^2 = \left(A\cdot\left(-\frac{4}{3}C\right) - 4F\right)^2 = \frac{16}{9}A^2C^2 + \frac{32}{3}ACF + 16F^2.$$

Similarly,

$$(\zeta(u+\alpha) - \eta)^2 = (A(2B+A) + \tfrac{4}{3}C)^2 = A^4 + 4A^3B + 4A^2B^2 + \frac{8}{3}A^2C + \frac{16}{3}ABC + \frac{16}{9}C^2.$$

$$\zeta(1-\zeta)(\eta-2u\zeta)^2 = 16A^3(1-A)B^2 + \frac{32}{3}A^2BC(1-A) + \frac{16}{9}AC^2(1-A).$$

$$4u\zeta^2(1-\zeta)^2(1-u) = 8BA^2(1-A)^2(1-2B).$$

Finally,

$$\begin{aligned}&16B(1-B) + \frac{16}{9}A^2C^2 + \frac{32}{3}ACF + 16F^2 + A^4 + 4A^3B + 4A^2B^2\\ &+ \frac{8}{3}A^2C + \frac{16}{3}ABC + \frac{16}{9}C^2 + \frac{16}{9}AC^2(1-A)\\ &+ \frac{32}{3}A^2BC(1-A) + 16A^3(1-A)B^2 \leq 8BA^2(1-A)^2(1-2B).\end{aligned}$$

The inequality (3.7) holds for all $\lambda \in [0,1]$.

Thus, by using Lemma 3.5, we conclude that

$$|r_5| \leq \frac{1}{5(1-\lambda)^2+4\lambda^2}. \tag{4.12}$$

□

Theorem 4.2. *Let $f \in \mathcal{A}$ be given in* (1.1)*. If $f \in \mathcal{S}^*(\varphi_H)$, then*

$$|r_3 - r_2^2| \leq \frac{1}{(3(1-\lambda)^2+2\lambda^2)}. \tag{4.13}$$

This is the best possible.

Proof. From (4.6) and (4.7),

$$r_2 = \frac{1}{4(1-2\lambda+2\lambda^2)}c_1,$$

$$r_3 = \frac{\left(\frac{1}{2}c_2 - \frac{1}{6}c_1^2\right) + \left(\frac{2\lambda(1-\lambda)}{16(1-2\lambda+2\lambda^2)^2}\right)c_1^2}{3(1-\lambda)^2+2\lambda^2},$$

$$r_3 - r_2^2 = \frac{\left(\frac{1}{2}c_2 - \frac{1}{6}c_1^2\right) + \left(\frac{2\lambda(1-\lambda)}{16(1-2\lambda+2\lambda^2)^2}\right)c_1^2}{3(1-\lambda)^2+2\lambda^2} - \left(\frac{1}{4(1-2\lambda+2\lambda^2)}c_1\right)^2,$$

$$r_3 - r_2^2 = \frac{\frac{1}{2}c_2 - \left[\frac{1}{6}c_1^2 + \left(\frac{2\lambda(1-\lambda)}{16(1-2\lambda+2\lambda^2)^2}\right)c_1^2\right]}{3(1-\lambda)^2+2\lambda^2} - \left(\frac{c_1^2}{16(1-2\lambda+2\lambda^2)^2}\right),$$

$$r_3 - r_2^2 = \frac{24(1-2\lambda+2\lambda^2)^2c_2 - \left[4(1-2\lambda+2\lambda^2)^2 + 6\lambda(1-\lambda) - 3(1-\lambda)^2 + 2\lambda^2\right]c_1^2}{48(1-2\lambda+2\lambda^2)^2 3(1-\lambda)^2+2\lambda^2},$$

$$r_3 - r_2^2 = \frac{24(1-2\lambda+2\lambda^2)^2\Big[c_2 - \left(\frac{1}{6} + \frac{\lambda(1-\lambda)}{4(1-2\lambda+2\lambda^2)} - \frac{(3-6\lambda+5\lambda^2)}{24(1-2\lambda+2\lambda^2)^2}\right)c_1^2\Big]}{48(1-2\lambda+2\lambda^2)^2 3(1-\lambda)^2+2\lambda^2}.$$

After cancellation of $24(1-2\lambda+2\lambda^2)^2$ with $48(1-2\lambda+2\lambda^2)^2$, we get

$$r_3 - r_2^2 = \frac{\Big[c_2 - \left(\frac{1}{6} + \frac{\lambda(1-\lambda)}{4(1-2\lambda+2\lambda^2)} - \frac{(3-6\lambda+5\lambda^2)}{24(1-2\lambda+2\lambda^2)^2}\right)c_1^2\Big]}{2[3(1-\lambda)^2+2\lambda^2]}.$$

By comparing with (3.2), we get

$$\theta = \frac{1}{6} + \frac{\lambda(1-\lambda)}{4(1-2\lambda+2\lambda^2)} - \frac{(3-6\lambda+5\lambda^2)}{24(1-2\lambda+2\lambda^2)^2}.$$

It is easy to verify that $0 < \theta < 1$ for all $\lambda \in [0,1]$. Hence, by Lemma 3.2,

$$|r_3 - r_2^2| \leq \frac{1}{3(1-\lambda)^2+2\lambda^2}.$$

□

Theorem 4.3. *Let $f \in \mathcal{A}$ be in the form* (1.1)*. If $f \in \mathcal{S}^*(\varphi_H)$, then*

$$|r_4 - r_2 r_3| \leq \frac{1}{4(1-2\lambda+2\lambda^2)}. \tag{4.14}$$

This inequality is the best possible.

Proof. From (4.6), (4.7), and (4.8), we get

$$r_2 = \frac{1}{4(1-2\lambda+2\lambda^2)}c_1,$$

$$r_3 = \frac{\left(\frac{1}{2}c_2 - \frac{1}{6}c_1^2\right) + \left(\frac{2\lambda(1-\lambda)}{16(1-2\lambda+2\lambda^2)^2}\right)c_1^2}{3(1-\lambda)^2+2\lambda^2},$$

$$r_4 = \frac{1}{4\left[(1-\lambda)^2+\lambda^2\right]}\Bigg[\frac{1}{2}c_3 + \frac{8\lambda^4-17\lambda^3-17\lambda^2+33\lambda-12}{12(1-2\lambda+2\lambda^2)(3(1-\lambda)^2+2\lambda^2)}c_1c_2 + \left(\frac{1}{36} + \frac{4\lambda(48\lambda^6-110\lambda^5+85\lambda^4-\lambda^3-61\lambda^2+50\lambda-15)}{192(1-2\lambda+2\lambda^2)^3(3(1-\lambda)^2+2\lambda^2)}\right)c_1^3\Bigg]$$

where, $P(\lambda) = 4\lambda(48\lambda^6-110\lambda^5+85\lambda^4-\lambda^3-61\lambda^2+50\lambda-15)$

$$|r_4 - r_2 r_3| = \left|\frac{1}{4(1-2\lambda+2\lambda^2)}\left[\frac{1}{2}c_3 + \frac{8\lambda^4-17\lambda^3-17\lambda^2+33\lambda-12}{12(1-2\lambda+2\lambda^2)(3(1-\lambda)^2+2\lambda^2)}c_1c_2\right.\right.$$

$$+\frac{1}{36}+\frac{P(\lambda)}{192(1-2\lambda+2\lambda^2)^3(3(1-\lambda)^2+2\lambda^2)}c_1^3\Bigg]$$
$$-\frac{1}{8(1-2\lambda+2\lambda^2)(3(1-\lambda)^2+2\lambda^2)}c_1c_2$$
$$-\left(\frac{-8(1-2\lambda+2\lambda^2)^2+6\lambda(1-\lambda)}{192(1-2\lambda+2\lambda^2)^3(3(1-\lambda)^2+2\lambda^2)}\right)c_1^3\Bigg|.$$

After some simplification, we obtain

$$|r_4-r_2r_3| = \frac{1}{8(1-2\lambda+2\lambda^2)}\left|c_3-2\left[\frac{-16\lambda^4+34\lambda^3+34\lambda^2-66\lambda+27}{6(3(1-\lambda)^2+2\lambda^2)}\right]c_1c_2\right.$$
$$\left.+\left[\frac{3P(\lambda)+16(1-2\lambda+2\lambda^2)^3(3(1-\lambda)^2+2\lambda^2)}{-3(32\lambda^4-64\lambda^3+58\lambda^2-26\lambda+8)}{192(1-2\lambda+2\lambda^2)^2(3(1-\lambda)^2+2\lambda^2)}\right]c_1^3\right|,$$

$$|r_4-r_2r_3| = \frac{1}{8(1-2\lambda+2\lambda^2)}\left|c_3-2Qc_1c_2+Tc_1^3\right|,$$

where,

$$Q = \frac{-16\lambda^4+34\lambda^3+34\lambda^2-66\lambda+27}{6(3(1-\lambda)^2+2\lambda^2)},$$

$$T = \left[\frac{3P(\lambda)+16(1-2\lambda+2\lambda^2)^3(3(1-\lambda)^2+2\lambda^2)}{-3(32\lambda^4-64\lambda^3+58\lambda^2-26\lambda+8)}{192(1-2\lambda+2\lambda^2)^2(3(1-\lambda)^2+2\lambda^2)}\right],$$

by using (3.3), we get

$$|r_4-r_2r_3| \le 2\left(\frac{1}{8(1-2\lambda+2\lambda^2)}\right),$$

$$|r_4-r_2r_3| \le \frac{1}{4(1-2\lambda+2\lambda^2)}.$$

□

Theorem 4.4. *Let $f \in \mathcal{A}$ be given by* (1.1)*. If $f \in \mathcal{S}^*(\varphi_H)$, then*

$$|r_2r_4-r_3^2| \le \frac{1}{(3(1-\lambda)^2+2\lambda^2)^2}. \tag{4.15}$$

This inequality is the best possible.

Proof. From (4.6), (4.7), and (4.8)

$$
\begin{aligned}
r_2 &= \frac{1}{4(1-2\lambda+2\lambda^2)}c_1,\\
r_3 &= \frac{\left(\frac{1}{2}c_2-\frac{1}{6}c_1^2\right)+\left(\frac{2\lambda(1-\lambda)}{16(1-2\lambda+2\lambda^2)^2}\right)c_1^2}{3(1-\lambda)^2+2\lambda^2},\\
r_4 &= \frac{1}{4\left[(1-\lambda)^2+\lambda^2\right]}\left[\frac{1}{2}c_3+\frac{8\lambda^4-17\lambda^3-17\lambda^2+33\lambda-12}{12(1-2\lambda+2\lambda^2)(3(1-\lambda)^2+2\lambda^2)}c_1c_2\right.\\
&\quad\left.+\left(\frac{1}{36}+\frac{4\lambda(48\lambda^6-110\lambda^5+85\lambda^4-\lambda^3-61\lambda^2+50\lambda-15)}{192(1-2\lambda+2\lambda^2)^3(3(1-\lambda)^2+2\lambda^2)}\right)c_1^3\right],\\
r_2r_4 &= \frac{1}{4(1-2\lambda+2\lambda^2)}\left[\frac{c_1}{4(1-2\lambda+2\lambda^2)}\left[\frac{1}{2}c_3+\left(\frac{8\lambda^4-17\lambda^3-17\lambda^2+33\lambda-12}{12(1-2\lambda+2\lambda^2)(3(1-\lambda)^2+2\lambda^2)}\right)c_1c_2\right.\right.\\
&\quad\left.\left.+\left(\frac{1}{36}+\frac{P(\lambda)}{192(1-2\lambda+2\lambda^2)^3(3(1-\lambda)^2+2\lambda^2)}\right)c_1^3\right],\\
r_2r_4 &= \frac{1}{16(1-2\lambda+2\lambda^2)^2}\left[\frac{1}{2}c_1c_3+\left(\frac{8\lambda^4-17\lambda^3-17\lambda^2+33\lambda-12}{12(1-2\lambda+2\lambda^2)(3(1-\lambda)^2+2\lambda^2)}\right)c_1^2c_2\right.\\
&\quad\left.+\left(\frac{1}{36}+\frac{P(\lambda)}{192(1-2\lambda+2\lambda^2)^3(3-\lambda^2)}\right)c_1^4\right],\\
r_3 &= \frac{\left(\frac{1}{2}c_2-\frac{1}{6}c_1^2\right)+\left(\frac{2\lambda(1-\lambda)}{16(1-2\lambda+2\lambda^2)^2}\right)c_1^2}{(3(1-\lambda)^2+2\lambda^2)},\\
r_3^2 &= \frac{\left(\frac{1}{2}c_2-\frac{1}{6}c_1^2+\frac{\lambda(1-\lambda)}{8(1-2\lambda+2\lambda^2)^2}c_1^2\right)^2}{\left[3(1-\lambda^2)+2\lambda^2\right]^2},\\
r_3^2 &= \frac{\frac{1}{4}c_2^2-2\left(\frac{1}{2}\right)\left(\frac{1}{6}-\frac{\lambda(1-\lambda)}{8(1-2\lambda+2\lambda^2)^2}\right)c_1^2c_2+c_1^4\left(\frac{1}{6}-\frac{\lambda(1-\lambda)}{8(1-2\lambda+2\lambda^2)^2}\right)^2}{\left[3(1-\lambda^2)+2\lambda^2\right]^2},\\
r_3^2 &= \frac{1}{[3(1-\lambda)^2+2\lambda^2]^2}\left[\frac{1}{4}c_2^2+\left(-\frac{1}{6}+\frac{\lambda(1-\lambda)}{8(1-2\lambda+2\lambda^2)^2}\right)c_2c_1^2\right.\\
&\quad\left.+\left(\frac{1}{36}-\frac{\lambda(1-\lambda)}{24(1-2\lambda+2\lambda^2)^2}\quad+\frac{\lambda^2(1-\lambda)^2}{64(1-2\lambda+2\lambda^2)^4}\right)c_1^4\right],\\
r_2r_4-r_3^2 &= \frac{1}{32(1-2\lambda+2\lambda^2)^2}c_1c_3\\
&\quad+\frac{1}{16(1-2\lambda+2\lambda^2)^2}\left[\left(\frac{8\lambda^4-17\lambda^3-17\lambda^2+33\lambda-12}{12(1-2\lambda+2\lambda^2)(3(1-\lambda)^2+2\lambda^2)}\right)c_1^2c_2\right.
\end{aligned}
$$

$$+\left(\frac{1}{36}+\frac{P(\lambda)}{192(1-2\lambda+2\lambda^2)^3(3(1-\lambda)^2+2\lambda^2)}\right)c_1^4\Bigg]$$
$$-\frac{1}{[3(1-\lambda)^2+2\lambda^2]^2}\Bigg[\left(-\frac{1}{12}+\frac{\lambda(1-\lambda)}{16(1-2\lambda+2\lambda^2)^2}\right)c_2c_1^2$$
$$+\left(\frac{1}{36}-\frac{\lambda(1-\lambda)}{24(1-2\lambda+2\lambda^2)^2}+\frac{\lambda^2(1-\lambda)^2}{64(1-2\lambda+2\lambda^2)^4}\right)c_1^4\Bigg]-\frac{1}{4[3(1-\lambda)^2+2\lambda^2]^2}c_2^2,$$

$$r_2r_4-r_3^2=\frac{c_1c_3}{32(1-2\lambda+2\lambda^2)}+\Bigg[\frac{8\lambda^4-17\lambda^3-17\lambda^2+33\lambda-12}{192(1-2\lambda+2\lambda^2)^3(3(1-\lambda)^2+2\lambda^2)}$$
$$+\frac{1}{12[3(1-\lambda)^2+2\lambda^2]^2}-\frac{\lambda(1-\lambda)}{16[3(1-\lambda)^2+2\lambda^2]^2(1-2\lambda+2\lambda^2)^2}\Bigg]c_1^2c_2$$
$$-\frac{c_2^2}{4[3(1-\lambda)^2+2\lambda^2]^2}+\Bigg[\frac{1}{576(1-2\lambda+2\lambda^2)^2}+\frac{P(\lambda)}{3072(1-2\lambda+2\lambda^2)^5(3(1-\lambda)^2+2\lambda^2)}$$
$$+\frac{\lambda(1-\lambda)}{24[3(1-\lambda)^2+2\lambda^2]^2(1-2\lambda+2\lambda^2)^2}-\frac{\lambda^2(1-\lambda)^2}{64[3(1-\lambda)^2+2\lambda^2]^2(1-2\lambda+2\lambda^2)^4}\Bigg]c_1^4.$$

Now, using Eqs (3.4) and (3.5) to define c_2 and c_3 in terms of c_1 and $c_1 = c$ $(0 \le c \le 2)$, and letting $\xi = 4 - c^2$ in Lemma (3.4), we obtain

$$|r_2r_4-r_3^2|\le\frac{1}{2304\beta^5\alpha^2}\Bigg|\Big[22\beta^3\alpha^2+6(8\lambda^4-17\lambda^3-17\lambda^2+33\lambda-12)\beta^2\alpha^2$$
$$+\frac{3}{4}P(\lambda)\alpha^2+24\lambda(1-\lambda)\beta^3-36\lambda^2(1-\lambda)^2\beta-112\beta^5\Big]c^4$$
$$+\Big[6(8\lambda^4-17\lambda^3-17\lambda^2+33\lambda-12)\beta^2\alpha^2$$
$$-72\lambda(1-\lambda)(1-2\lambda+2\lambda^2)^3(3-\lambda^2)-192(1-2\lambda+2\lambda^2)^5(3-\lambda^2)\Big]c^2x\xi$$
$$-\Big[18\beta^3\alpha^2\Big]c^2x^2\xi-\Big[\beta^5\Big]x^2\xi^2+\Big[36\beta^3\alpha^2\Big]c\xi(1-|x|^2)\delta\Bigg|.$$

Where

$$\alpha = 3(1-\lambda)^2+2\lambda^2, \beta = (1-2\lambda+2\lambda^2).$$

By using $|\delta| \le 1$ and $|x| = b \le 1$ and after applying triangular inequality, we get

$$|r_2r_4-r_3^2|\le\frac{1}{2304\beta^5\alpha^2}\Bigg|\Big[22\beta^3\alpha^2+6(8\lambda^4-17\lambda^3-17\lambda^2+33\lambda-12)\beta^2\alpha^2$$
$$+\frac{3}{4}P(\lambda)\alpha^2+24\lambda(1-\lambda)\beta^3-36\lambda^2(1-\lambda)^2\beta\eta-112\beta^5\Big]c^4$$
$$+\Big[36\beta^3\alpha^2+6(8\lambda^4-17\lambda^3-17\lambda^2+33\lambda-12)\beta^2\alpha^2$$
$$-72\lambda(1-\lambda)\beta^3-192\beta^5\Big]c^2b\xi$$
$$-\Big[18\beta^3\alpha^2\Big]c^2b^2\xi-\Big[144\beta^5\Big]b^2\xi^2+\Big[36\beta^3\alpha^2\Big]c\xi(1-|b|^2)\Bigg| =: E(c,b).$$

Now, partially differentiating E(c,b) with respect to b, we obtain

$$E'(c,b) = \begin{bmatrix} 36\beta^3\alpha^2 + 6(8\lambda^4 - 17\lambda^3 - 17\lambda^2 + 33\lambda - 12)\beta^2\alpha^2 \\ -72\lambda(1-\lambda)\beta^3 - 192\beta^5 \end{bmatrix} c^2\xi \\ -2\left[18\beta^3\alpha^2\right]cb\xi - 2\left[144\beta^5\right]b\xi^2.$$

We examine that $E'(c,b) \geq 0$ for all $\lambda \in [0,1]$, so we have $E(c,b) \leq E(c,1)$. Replacing $b = 1$ gives

$$|r_2r_4 - r_3^2| \leq \frac{1}{2304\beta^5\alpha^2}\Bigg|\Big[22\beta^3\alpha^2 + 6(8\lambda^4 - 17\lambda^3 - 17\lambda^2 + 33\lambda - 12)\beta^2\alpha^2 \\ + \frac{3}{4}P(\lambda)\alpha^2 + 24\lambda(1-\lambda)\beta^3 - 36\lambda^2(1-\lambda)^2\beta - 112\beta^5\Big]c^4 \\ + \Big[36\beta^3\alpha^2 + 6(8\lambda^4 - 17\lambda^3 - 17\lambda^2 + 33\lambda - 12)\beta^2\alpha^2 \\ - 72\lambda(1-\lambda)\beta^3 - 192\beta^5\Big]c^2\xi \\ - \Big[18\beta^3\alpha^2\Big]c^2\xi - \Big[144\beta^5\Big]\xi^2\Bigg| =: E(c,1).$$

$E'(c,1) < 0$, so $E(c,1)$ is a decreasing function and achieves maximum value at $c = 0$ for $\xi \in [0,1]$, $c \in [0,2]$, and $\lambda \in [0,1]$.

$$|r_2r_4 - r_3^2| \leq \frac{1}{2304\beta^5\alpha^2}\Big|[144\beta^5](16)\Big|,$$

$$|r_2r_4 - r_3^2| \leq \frac{1}{(3(1-\lambda)^2 + 2\lambda^2)^2}.$$

□

Theorem 4.5. *Let $f \in \mathcal{A}$ as given in* (1.1)*. If $f \in \mathcal{S}^*(\varphi_H)$, then*

$$|\mathcal{H}_{3,1}(f)| \leq \frac{\Omega(\lambda)}{48D_5\alpha^2\beta^2}. \tag{4.16}$$

Proof. Using triangle inequality,

$$|\mathcal{H}_{3,1}(f)| \leq |r_3||r_2r_4 - r_3^2| + |r_4||r_4 - r_2r_3| + |r_5||r_3 - r_2^2|.$$

By using (4.10), (4.15), (4.14), (4.12), and (4.13), we have

$$\left|\mathcal{H}_{3,1}(f)\right| \leq \left(\frac{1}{3((1-\lambda)^2 + 2\lambda^2)}\right)\left(\frac{1}{(3(1-\lambda)^2 + 2\lambda^2)^2}\right) \\ + \left(\frac{1}{4[(1-\lambda)^2 + \lambda^2]}\right)\left(\frac{1}{4(1 - 2\lambda + 2\lambda^2)}\right) \\ + \left(\frac{1}{5(1-\lambda)^2 + 4\lambda^2}\right)\left(\frac{1}{3(1-\lambda)^2 + 2\lambda^2}\right).$$

After some calculation, we get

$$|\mathscr{H}_{3,1}(f)| \leq \frac{\Omega(\lambda)}{48D_5\alpha^2\beta^2},$$

where,

$$\Omega(\lambda) = 16D_5\beta^2 + 3D_5\alpha^2\gamma + 6\alpha^2\beta\gamma + 48\alpha\beta\gamma,$$

$$\beta = (1-\lambda)^2 + \lambda^2, \alpha = 3(1-\lambda)^2 + 2\lambda^2, \gamma = (1-\lambda)^2 + 2\lambda^2.$$

□

The estimate obtained for the third Hankel determinant $|H_{3,1}(f)|$ is derived by applying the triangle inequality together with the coefficient bounds established in Theorems 4.2–4.4. Since equality in all intermediate inequalities cannot generally be attained simultaneously, the exact extremal function corresponding to the bound of $|H_{3,1}(f)|$ is not explicitly determined. Therefore, the obtained result should be regarded as an upper bound estimate for the considered class.

Corollary 4.1. *For,*

$$\mathcal{S}^*(\lambda) = \left\{ f \in \mathcal{K} : (1-\lambda)(f'(z))^{1-\lambda} + \lambda\left(\frac{2zf'(z)}{f(z)-f(-z)}\right)^{\lambda} \prec 1 + z + \frac{z^2}{3} - \frac{z^3}{9}, \forall z \in \mathfrak{D} \right\}.$$

We have two domains of $\mathcal{S}^*(\lambda)$ for particular values of λ.

(1) For $\lambda = 0$, we get bounded turning domain

$$\mathcal{S}^*(\lambda) = \left\{ f \in \mathcal{K} : f'(z) \prec 1 + z + \frac{z^2}{3} - \frac{z^3}{9}, \forall z \in \mathfrak{D} \right\}.$$

(2) For $\lambda = 1$, we get symmetric starlike domain

$$\mathcal{S}^*(\lambda) = \left\{ f \in \mathcal{K} : \frac{2zf'(z)}{f(z)-f(-z)} \prec 1 + z + \frac{z^2}{3} - \frac{z^3}{9}, \forall z \in \mathfrak{D} \right\}.$$

5. Applications of Hankel determinants in texture enhancement

Digital images [27] play a vital role in fields, such as artificial intelligence and virtual reality, and perform several types of adjustment, including image capture, enhancement, and transmission process. A significant aspect of digital image processing is texture enhancement, which improves edge contrast and facilitates edge detection, splitting an image into different regions based on texture homogeneity. Texture enhancement also plays a crucial role in real world applications such as in biometrics for security purposes and medical imaging for the detection of tumors and skin cancer disease to find lesions.

In medical image processing, texture enhancement is used to improve the visual quality of somatic structures and lesion boundaries for better diagnostic analysis. We propose a novel texture

enhancement algorithm that utilizes convolution masks of Hankel determinants in multi directions. These estimated Hankel determinants play a significant role in image processing because they contain important geometric and structural information for constructing convolution masks for texture enhancement. By integrating these Hankel determinant based approaches into an enhancement framework, the proposed method improves edge and texture visibility and preserves structural integrity.

Image quality is assessed using different quality metrics like contrast, correlation, energy, homogeneity, and entropy [20].

Contrast measures the difference between pixel intensities,

$$C_{ont} = \sum_{i} \sum_{j} (i-j)^k P_{i,j}.$$

Correlation measures how a pixel is correlated with its neighbor;

$$C_{orr} = \frac{\sum_i \sum_j ij P_{a,b} - \mu_i \mu_j}{\sigma_i \sigma_j}.$$

Energy measures the texture uniformity of an image;

$$E_{enr} = \sum_{i,j} \left(P_{i,j}\right)^2.$$

Homogeneity measures the closeness of GLCM elements with diagonals. A high value of homogeneity indicates that all pixels have the same value;

$$H = \sum_{a} \sum_{b} \frac{P_{a,b}}{1+|a-b|}.$$

Entropy measures the disorder of pixel intensities;

$$E_{ent} = -\sum_{a} \sum_{b} P_{a,b} \ln\left(P_{a,b}\right).$$

Now, we find Hankel determinants for class $S^*_{(\varphi_H)}$ by substituting different values of λ in (4.13), (4.15) and (4.16) and we represent $|\mathscr{H}_{2,1}(f)|$, $|\mathscr{H}_{2,2}(f)|$, and $|\mathscr{H}_{3,1}(f)|$ as $\hbar_1$, $\hbar_2$, and $\hbar_3$, respectively. The 8 mask windows are not selected randomly, and these masks are built on the values of Hankel determinants associated from λ-generalized Sakaguchi type functions. These Hankel determinants help improve lesion boundaries, reduce background noise and enhance pigmented boundaries.

5.1. Proposed algorithm

In this section, we introduces the novel algorithm using Hankel determinants for the class $S^*_{(\varphi_H)}$. We use h_1, h_2, and h_3 found at $\lambda = 0.3$. Different values of λ are examined over the interval $[0, 1]$ to analyze the stability and effectiveness of our proposed algorithm. Among all these values, $\lambda = 0.3$ achieves the balanced enhancement performance and better preservation of structural details. Therefore, $\lambda = 0.3$ is selected for the proposed algorithm. The proposed masks are constructed using the first three Hankel determinant values $\hbar_1 = 0.6060$, $\hbar_2 = 0.3673$, and $\hbar_3 = 2.0067$ obtained at $\lambda = 0.3$. The utilization of Hankel determinants in mask windows improves edge preservation and texture enhancement.

$$\mathscr{H}_{\mathbb{S}}(m,n) = \mathbb{M} * \mathscr{H}_{\mathbb{O}}(m,n),$$

where,

- $\mathbb{M}$ denotes the 3×3 mask window.
- $*$ is the convolution operation.
- $\mathscr{H}_{\mathscr{E}}$ denotes enhanced image.
- $\mathscr{H}_{\mathscr{O}}(m, n)$ denotes input image.

(a) h_{0° (Horizontal/Right)

$-h_1$	0	h_1
h_1	h_2	h_3
h_1	0	$-h_1$

(b) h_{45° (Diagonal Up-Right)

0	$-h_1$	h_3
0	h_2	0
h_1	0	$-h_1$

(c) h_{90° (Vertical/Up)

0	h_3	$-h_1$
0	h_2	$-h_1$
h_1	h_1	0

(d) h_{135° (Diagonal Up-Left)

h_3	0	$-h_1$
0	h_2	0
$-h_1$	0	h_1

(e) h_{180° (Horizontal/Left)

0	h_1	0
h_3	h_2	h_1
0	0	h_1

(f) h_{225° (Diagonal Down-Left)

$-h_1$	0	h_1
0	h_2	0
h_3	0	$-h_1$

(g) h_{270° (Vertical/Down)

0	h_1	$-h_1$
0	h_2	$-h_1$
0	h_3	h_1

(h) h_{315° (Diagonal Down-Right)

h_1	0	$-h_1$
0	h_2	0
$-h_1$	0	h_3

The proposed texture enhancement algorithm involves 6 steps.
Step 1: Convert original images to lab color image.
Step 2: Apply K-mean clustering on lab color image to get a segmented image and then convert it into gray-scale to produce a texture image.
Step 3: Calculate the GLCM of the texture image.
Step 4: Place a mask window over 3×3 pixel size.
Step 5: Apply the convolution of mask window over the texture image in 8 different directions and take maximum of all directions to produce an enhanced texture image.
Step 6: Calculate the GLCM and texture feature for an enhanced texture image.

6. Comparative analysis

Comparative analysis ensures the strength of the proposed texture enhancement algorithm since the proposed method provides better texture enhancement and edge detection compared with texture images produced using the algorithm proposed by Aldi et al. [20]. The same image dataset, preprocessing procedure, and K-means segmentation method are used for the proposed method and the Aldi et al. method. For the better enhancement of lesion boundary, additional processing is

performed through the convolution of Hankel determinants with the image pixels of the segmented image. In earlier studies, [28–31] algorithms were based on histogram equalization, logarithmic transform coefficients, and discrete cosine enhancement methods that use coefficient bounds for image enhancement. In contrast, our method utilizes Hankel determinants derived from the subclass of λ generalized Sakaguchi type functions associated with the image domain of $\varphi_{H(z)}$. In this study, we develop a novel algorithm that convolves the input image with Hankel determinants using 8 directional matrices to produce an enhanced texture image. Our method illustrates significant improvements in texture quality across datasets, as shown in Table 2, while the texture images produced by the algorithm used in [20] do not contain clear structural details. Utilizing this algorithm, a texture-enhanced image is produced with clear edges of a segmented lesion boundary. This improvement in edges leads to better texture features, and produces clearer images with less noise.

The above proposed texture enhancement algorithm is tested on dermoscopy images for skin cancer analysis. We use JPG images of Basal Cell Carcinoma, Dermatofibroma, Melanoma, Pigmented Benign Keratosis, and Vascular Lesion obtained from the Kaggle repository [32], which are converted into texture enhanced images, as shown in Figures 1–5. These figures produce sharp edge boundaries, enhanced lesion structures, and reduced background noise while preserving structural integrity compared with the method of Aldi et al. [20]. The best results were achieved at $\lambda = 0.3$ with respect to texture features.

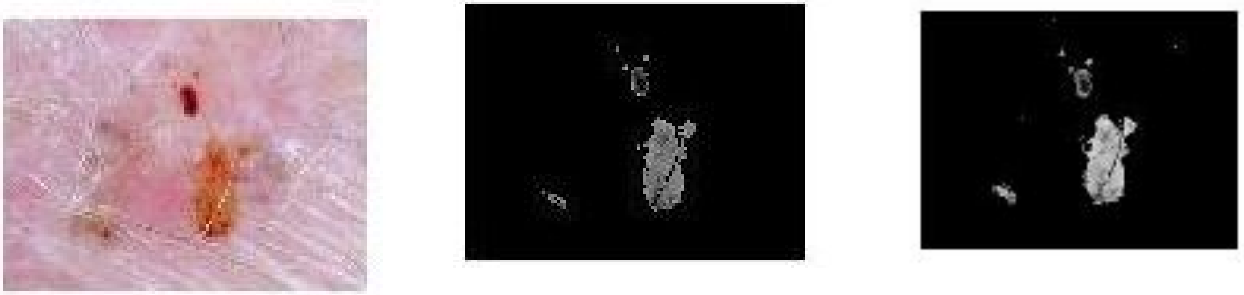

Original image

Texture image using the method by Aldi et al. [20]

Texture image enhancement using the proposed algorithm

Figure 1. Texture enhancement of basal cell carcinoma.

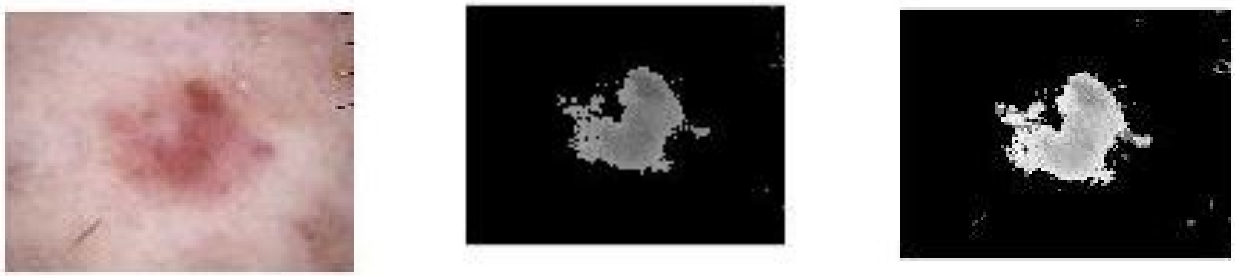

Original image | Texture image using the method by Aldi et al. [20] | Texture image enhancement using the proposed algorithm

Figure 2. Texture enhancement of dermatofiborma.

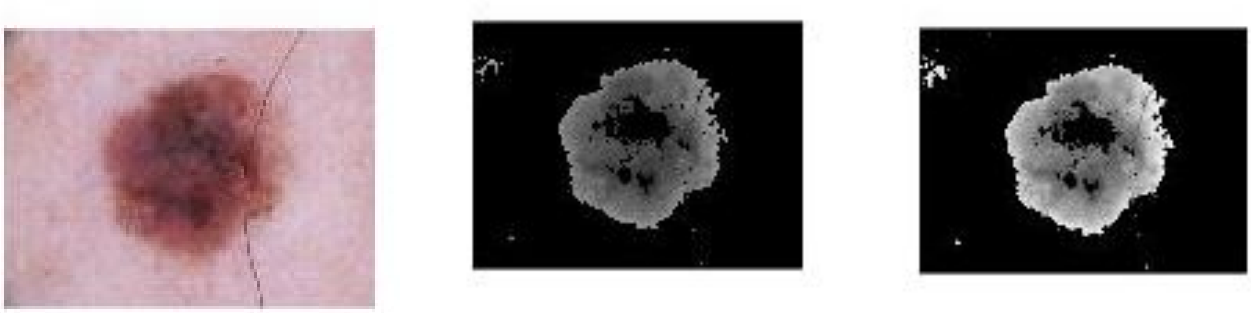

Original image | Texture image using the method by Aldi et al. [20] | Texture image enhancement using the proposed algorithm

Figure 3. Texture enhancement of melanoma.

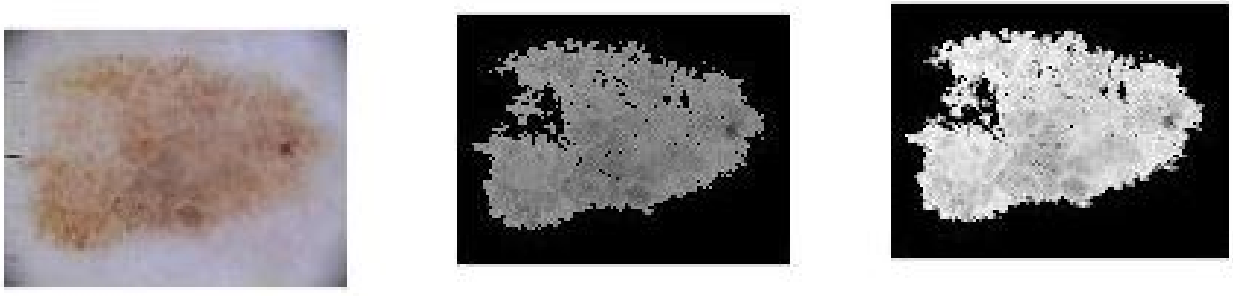

Original image | Texture image using the method by Aldi et al. [20] | Texture image enhancement using the proposed algorithm

Figure 4. Texture enhancement of pigmented benign keratosis.

Original image

Texture image using the method by Aldi et al. [20]

Texture image enhancement using the proposed algorithm

Figure 5. Texture enhancement of vascular lesions.

By comparing enhanced images produced by our proposed algorithm and the algorithm used in [20], we observe that proposed texture enhancement algorithm extracts both texture features and performs edge analysis, and due to the convolution mask, it produces clear object boundaries and less background noise, while the algorithm used in [20] focuses on only the statistical texture feature, and the resulting image looks softer due to the lack of a convolution mask.

Table 1 shows the quality metrics of the proposed algorithm and Aldi et al.'s method. In image enhancement, contrast is not only an indicator of quality. The increase value of contrast and entropy, particularly for Pigmented Benign Keratosis, ensures that the method enhances texture features rather than increase only intensity variation. A higher value of correlation shows the preservation of structural integrity, which enhances the edges of the pigmented structure. A higher value of energy represents that the texture is more organized, which means it is easy to diagnose skin lesions. A slight decrease in homogeneity demonstrates sharp edges and reduced over smoothing. A higher value of entropy represents increased texture information, which shows the improvement in visibility of diagnostic features. Overall, the performance of quality metrics indicates that the proposed method achieves a balanced enhancement between contrast, correlation, and entropy rather than maximizing a single metric.

Table 1. Comparative analysis of texture feature: Second order GLCM vs. the proposed method.

Images	Methods	Contrast	Correl.	Energy	Homog.	Entropy
Basal Cell Carcinoma	Aldi et al. [20]	0.0753	0.9291	0.8978	0.9921	0.2713
	Proposed Method	0.0577	0.9699	0.8985	0.9888	0.3486
Dermatofibroma	Aldi et al. [20]	0.1876	0.9558	0.6995	0.9857	0.4756
	Proposed Method	0.1157	0.9816	0.7762	0.9813	0.6592
Melanoma	Aldi et al. [20]	0.0866	0.9746	0.5448	0.9912	0.8611
	Proposed Method	0.0635	0.9911	0.6045	0.9849	1.0456
Pigmented Benign Keratosis	Aldi et al. [20]	0.1666	0.9763	0.3734	0.9758	1.1651
	Proposed Method	0.2701	0.9846	0.3536	0.9496	1.5797
Vascular Lesion	Aldi et al. [20]	0.3845	0.9082	0.3024	0.9595	1.4950
	Proposed Method	0.3151	0.9429	0.3063	0.9333	1.7933

The proposed algorithm mainly focuses on preserving structural integrity, edge visibility, and rich texture information through directional convolution masks derived from Hankel determinants. (FSIM) is considered a suitable image quality assessment in this context because it evaluates edge preservation, structural similarity, and texture consistency using gradient and phase congruency. The improvements observed in FSIM indicate the enhancement behavior of dermoscopy images. Therefore, FSIM is considered to be served as a single quality metric for evaluating the effectiveness of our proposed method. Table 2 shows the enhancement behavior of different types of skin lesions by manifesting the best results of FSIM achieved through the proposed method.

Table 2. Comparison of single quality assessment values.

Images	Methods	FSIM
Basal Cell Carcinoma	Aldi et al. [20]	0.9043
	Proposed Method	0.9083
Dermatofibroma	Aldi et al. [20]	0.9398
	Proposed Method	0.9502
Melanoma	Aldi et al. [20]	0.9617
	Proposed Method	0.9709
Pigmented Benign Keratosis	Aldi et al. [20]	0.9084
	Proposed Method	0.9349
Vascular Lesion	Aldi et al. [20]	0.8679
	Proposed Method	0.8712

Moreover, other images of skin disease were also examined through this novel texture enhancement algorithm to validate the proposed algorithm. Different types of skin diseases can be analyzed easily due to improved geometric structure and smoother texture enhancement. The dataset used in Figure 6 are also obtained from the Kaggle repository [32]. Figure 6 indicates that the improvement in texture quality and smooth edge detection of these images is visible. This ensures the effectiveness of the

proposed algorithm, as the texture features become more enhanced, resulting in an enhanced texture image with improved lesion boundaries and structural visibility.

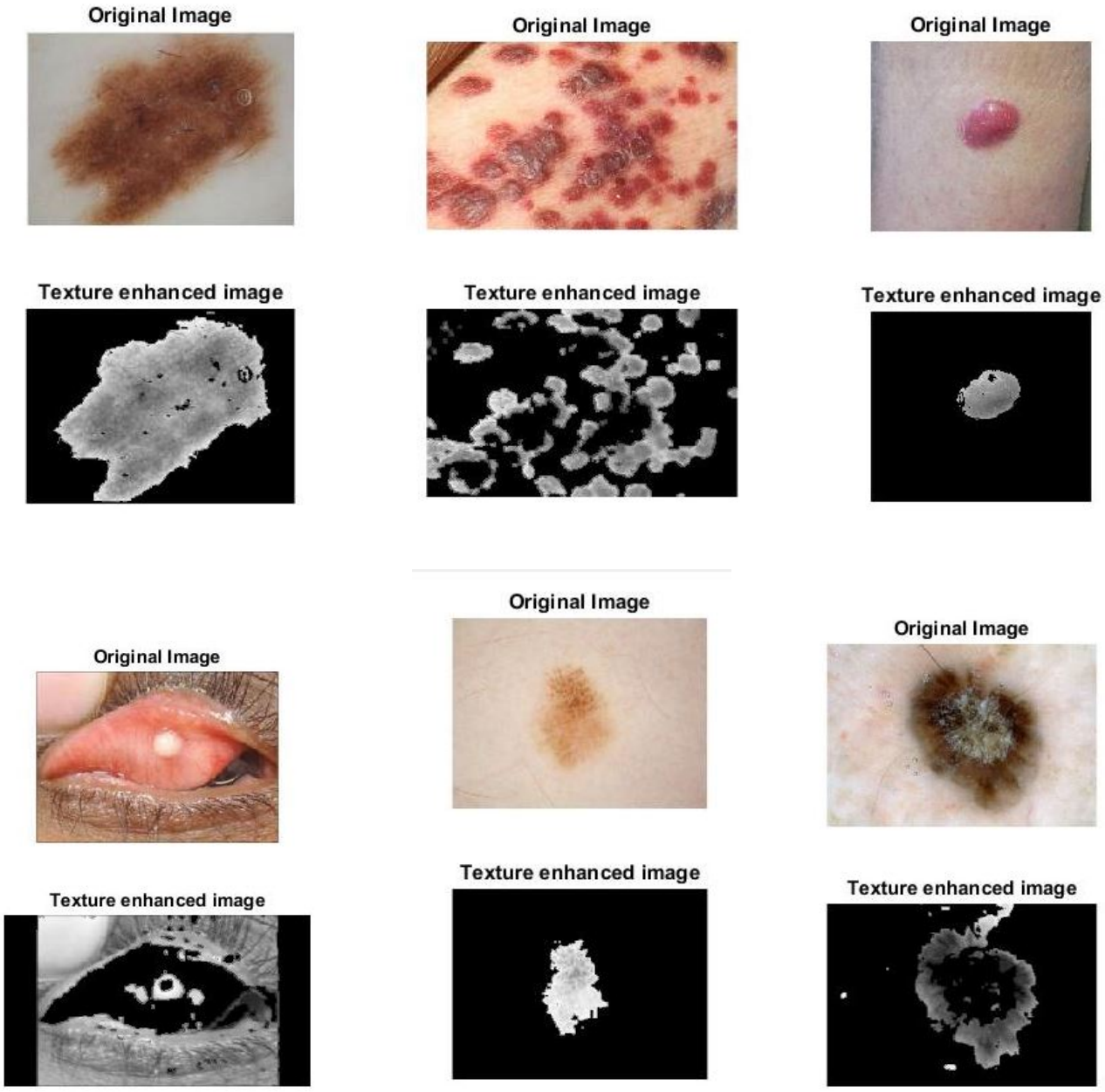

Figure 6. Enhancement of skin diseases using the proposed algorithm.

The quality metrics computed in Table 3 also prove the effectiveness of our proposed algorithm by showing better performance of the metrics across different skin lesion images. We have further demonstrated the effectiveness and validity of our proposed algorithm by evaluating FSIM as a single quality metric. Table 4 shows better results of FSIM, which proves better preservation of edge details, structural integrity, and richer texture information of dermoscopy images. This shows the general robustness of our method and the effectiveness of our proposed algorithm.

Table 3. Quality metrics of different skin lesions.

Images	Categories of images	Contrast	Correl.	Energy	Homog.	Entropy
Actinic keratosis	Original Image	0.0580	0.9855	0.2605	0.9713	1.6831
	Texture-enhanced image	0.1515	0.9854	0.3412	0.9605	1.6288
Kaposi Sacroma	Original Image	0.2452	0.9367	0.1264	0.8861	2.3807
	Texture-enhanced image	0.4687	0.9443	0.4094	0.9055	1.7561
Merkel cell carcinoma	Original Image	0.0577	0.9526	0.3852	0.9712	1.2930
	Texture-enhanced image	0.0124	0.9919	0.8989	0.9968	0.2969
Sebaceous gland carcinoma	Original Image	0.2903	0.9444	0.1382	0.9032	2.3278
	Texture-enhanced image	0.2887	0.9712	0.1988	0.9141	2.2318
Seborrheic keratosis	Original Image	0.2986	0.9483	0.5364	0.9852	0.8521
	Texture-enhanced image	0.0620	0.9889	0.8479	0.9899	0.4382
Squamous cell carcinoma	Original Image	0.0919	0.9857	0.2803	0.9545	1.9089
	Texture-enhanced image	0.0770	0.9667	0.7043	0.9779	0.8445

Table 4. Comparison of single quality assessment values among skin lesions.

Images	Methods	FSIM
Actinic keratosis	Aldi et al. [20]	0.9203
	Proposed Method	0.9405
Kaposi Sarcoma	Aldi et al. [20]	0.7600
	Proposed Method	0.7744
Merkel cell carcinoma	Aldi et al. [20]	0.9550
	Proposed Method	0.9563
Sebaceous gland carcinoma	Aldi et al. [20]	0.8843
	Proposed Method	0.9107
Seborrheic keratosis	Aldi et al. [20]	0.9609
	Proposed Method	0.9667
Squamous cell carcinoma	Aldi et al. [20]	0.8975
	Proposed Method	0.9023

7. Conclusions

Our main goal of this paper is to develop a novel algorithm using estimated Hankel determinants to obtain an enhanced version of the segmented image. In this study, we establish the sharp

coefficient inequalities through subordination for the subclass of λ-generalized Sakaguchi-type functions associated with the image domain of $\varphi_H(z)$ and find second and third order Hankel determinants for class $\mathcal{S}^*(\varphi_H)$.

Here, we develop a novel algorithm that utilizes the convolution of a mask window of the Hankel determinant with image pixels to enhance images. The experimental results demonstrate better texture features and clear edges of different dermoscopy images compared to the texture image of Aldi et al. [20]. Our proposed method also reduces noise while preserving geometric properties that lead to producing an enhanced image.

List of symbols and notations

$\mathcal{C}$	Complex plane
$\mathbb{N}$	Natural Numbers
$\mathfrak{R}$	Real part of Complex numbers
$\mathfrak{D}$	Open Unit Disc
w	Schwarz Function
$\mathcal{K}$	Class of Normalized Univalent Functions
$\mathcal{P}$	Class of Caratheodory Functions
$\prec$	Subordination
$*$	Convolution
$\mathcal{H}_{m,n}(f)$	Hankel Determinants of order m
$\mathcal{S}^*$	Class of Starlike Functions
$\mathcal{C}$	Class of Convex Functions
$\mathcal{S}^*_\lambda$	Class of λ generalized Sakaguchi type functions w.r.t. Symmetric Point
$\mathcal{S}^*(\varphi_H)$	subclass of λ generalized Sakaguchi type functions associated with symmetric domain.
r_n	coefficient of $\mathcal{S}^*(\varphi_H)$.
c_n	coefficients of Caratheodory functions.
λ	A real parameter in [0,1].
α	$3(1-\lambda)^2 + 2\lambda^2$.
β	$1 - 2\lambda + 2\lambda^2$.
$\mathcal{H}_E(m,n)$	Enhanced Image
$\mathcal{H}_O(m,n)$	Input Image
$\mathbb{M}$	3×3 Mask Window

Author contributions

Bushra Kanwal: Conceptualization, data curation, formal analysis, investigation, methodology, software, supervision, validation, writing review and editing; Kashaf Fatima: Conceptualization, data curation, formal analysis, investigation, methodology, software, validation, writing original draft; Dalal Alhwikem: Conceptualization, data curation, formal analysis, methodology, supervision, validation, writing original draft, writing review and editing; Sheza El-Deeb: Conceptualization, data curation,

formal analysis, investigation, methodology, supervision, writing original draft, writing review and editing. All authors have read and approved the final version of the manuscript for publication.

Use of Generative-AI tools declaration

The authors declare that they have not used Artificial Intelligence (AI) tools in the creation of this article.

Data availability

Source file of dermoscopy images.

Acknowledgments

The researchers would like to thank the Deanship of Graduate Studies and Scientific Research at Qassim University for financial support (QU-APC-2026).

Conflict of interest

The authors declare no conflicts of interest.

References

1. P. L. Duren, *Univalent functions*, New York: Springer, 1983.
2. C. Pommerenke, On the Hankel determinants of univalent functions, *Mathematika*, **14** (1967), 108–112. https://doi.org/10.1112/S002557930000807X
3. J. W. Noonan, D. K. Thomas, On the second Hankel determinant of areally mean p-valent functions, *Trans. Amer. Math. Soc.*, **223** (1976), 337–346. https://doi.org/10.2307/1997533
4. W. Hu, J. Deng, Hankel determinants, Fekete–Szegö inequality, and estimates of initial coefficients for certain subclasses of analytic functions, *AIMS Mathematics*, **9** (2024), 6445–6467. https://doi.org/10.3934/math.2024314
5. A. W. Goodman, On uniformly starlike functions, *J. Math. Anal. Appl.*, **155** (1991), 364–370. https://doi.org/10.1016/0022-247X(91)90006-L
6. E. Lindelöf, Mémoire sur certaines inégalités dans la théorie des fonctions monogènes et sur quelques propriétés nouvelles de ces fonctions dans le voisinage d'un point singulier essentiel, *Acta. Soc. Sci. Fenn.*, **35** (1909), 1–35.
7. W. Rogosinski, G. Szegö, Über die Abschnitte von Potenzreihen, die in einem Kreise beschränkt bleiben, *Math. Z.*, **28** (1928), 73–94. https://doi.org/10.1007/BF01181146
8. A. W. Goodman, *Univalent functions*, Tampa, FL: Mariner Publishing Company, 1983.
9. P. Sunthrayuth, I. Aldawish, M. Arif, M. Abbas, S. El-Deeb, Estimation of the second-order Hankel determinant of logarithmic coefficients for two subclasses of starlike functions, *Symmetry*, **14** (2022), 2039. https://doi.org/10.3390/sym14102039

10. A. A. Lupaş, A. S. Tayyah, J. Sokół, Sharp bounds on Hankel determinants for starlike functions defined by symmetry with respect to symmetric domains, *Symmetry*, **17** (2025), 1244. https://doi.org/10.3390/sym17081244

11. L. Shi, M. Arif, J. Iqbal, K. Ullah, S. M. Ghufran, Sharp bounds of Hankel determinant on logarithmic coefficients for functions starlike with exponential function, *Fractal Fract.*, **6** (2022), 645. https://doi.org/10.3390/fractalfract6110645

12. Q. A. Shakir, A. S. Tayyah, D. Breaz, L. I. Cotîrlă, E. Rapeanu, F. M. Sakar, Upper bounds of the third Hankel determinant for bi-univalent functions in crescent-shaped domains, *Symmetry*, **16** (2024), 1281. https://doi.org/10.3390/sym16101281

13. M. F. Khan, M. Abaoud, Coefficient inequalities and Hankel determinant for a new subclass of q-starlike functions, *J. Inequal. Appl.*, **2025** (2025), 95. https://doi.org/10.1186/s13660-025-03337-z

14. A. Riaz, M. Raza, D. K. Thomas, Hankel determinants for starlike and convex functions associated with sigmoid functions, *Forum Math.*, **34** (2021), 137–156. https://doi.org/10.1515/forum-2021-0188

15. B. Khan, Z. Orouji, A. Ebadian, Some results related to Booth lemniscate and integral operators, *Fractal Fract.*, **9** (2025), 271. https://doi.org/10.3390/fractalfract9050271

16. K. S. Sundari, B. S. Keerthi, Enhancing the quality of low-light images via the coefficient bounds derived for a subclass of Sakaguchi-type function, *J. Image Video Proc.*, **2025** (2025), 4. https://doi.org/10.1186/s13640-025-00663-6

17. P. Hari, B. Sruthakeerthi, Digital image processing using coefficient of Sakaguchi kind functions defined in Limacon-shaped domain with power law transformation, *Contemp. Math.*, **5** (2024), 2680–2692. https://doi.org/10.37256/cm.5320244489

18. R. Kamali, S. Prema, A. S. Ajay Shrikaanth, V. Govindan, M. Donganont, Image edge detection enhancement using coefficient estimates for classes of quasi-subordination: Fekete–Szegö problems, *Eur. J. Pure Appl. Math.*, **18** (2025), 6632. https://doi.org/10.29020/nybg.ejpam.v18i4.6632

19. B. Kanwal, A. Iman, S. Kanwal, A. K. Alkhalifa, Estimation of Hankel inequalities of symmetric starlike functions in crescent-shaped domain and their application in image processing, *Sci. Rep.*, **15** (2025), 27402. https://doi.org/10.1038/s41598-025-12935-2

20. F. Aldi, Sumijan, Extraction of shape and texture features of dermoscopy image for skin cancer identification, *Sinkron: J. Penelitian Teknik Inform.*, **8** (2024), 650–660. https://doi.org/10.33395/sinkron.v8i2.13557

21. P. Sunthrayuth, Y. Jawarneh, M. Naeem, N. Iqbal, J. Kafle, Some sharp results on coefficient estimate problems for four-leaf-type bounded turning functions, *J. Funct. Spaces*, **2022** (2022), 8356125. https://doi.org/10.1155/2022/8356125

22. R. J. Libera, E. J. Złotkiewicz, Coefficient bounds for the inverse of a function with derivative in P, *Proc. Amer. Math. Soc.*, **87** (1983), 251–257. https://doi.org/10.1090/S0002-9939-1983-0681830-8

23. C. Pommerenke, A. Vasil'ev, Angular derivatives of bounded univalent functions and extremal partitions of the unit disk, *Pacific J. Math.*, **206** (2002), 425–450. https://doi.org/10.2140/pjm.2002.206.425

24. O. S. Kwon, A. Lecko, Y. J. Sim, On the fourth coefficient of functions in the Carathéodory class, *Comput. Methods Funct. Theory*, **18** (2018), 307–314. https://doi.org/10.1007/s40315-017-0229-8

25. R. J. Libera, E. J. Złotkiewicz, Early coefficients of the inverse of a regular convex function, *Proc. Amer. Math. Soc.*, **85** (1982), 225–230. https://doi.org/10.1090/S0002-9939-1982-0652447-5

26. V. Ravichandran, S. Verma, Bound for the fifth coefficient of certain starlike functions, *C. R. Math.*, **353** (2015), 505–510. https://doi.org/10.1016/j.crma.2015.03.003

27. L. S. G. Kovásznay, H. M. Joseph, Image processing, *Proc. IRE*, **43** (1955), 560–570. https://doi.org/10.1109/JRPROC.1955.278100

28. F. Hossain, M. R. Alsharif, Image enhancement based on logarithmic transform coefficient and adaptive histogram equalization, In: *2007 International conference on convergence information technology*, 2007. https://doi.org/10.1109/ICCIT.2007.258

29. K. Panetta, J. Xia, S. Agaian, Color image enhancement based on the discrete cosine transform coefficient histogram, *J. Electron. Imaging*, **21** (2012), 021117. https://doi.org/10.1117/1.JEI.21.2.021117

30. L. Lu, Y. Zhou, K. Panetta, S. Agaian, Comparative study of histogram equalization algorithms for image enhancement, *Proc. SPIE*, **7708** (2010), 770811. https://doi.org/10.1117/12.853502

31. J. Xia, K. Panetta, S. Agaian, Color image enhancement algorithm based on logarithmic transform coefficient histogram, *Proc. SPIE*, **7870** (2011), 78700Y. https://doi.org/10.1117/12.872418

32. A. Katanskiy, *Skin Cancer ISIC*, Kaggle, 2019. Available from: `https://www.kaggle.com/datasets/nodoubttome/skin-cancer9-classesisic`

AIMS Press